New Phytologist

Research

An interdomain network: the endobacterium of a mycorrhizal fungus promotes antioxidative responses in both fungal and plant hosts

Candida Vannini[1], Andrea Carpentieri[2], Alessandra Salvioli[3], Mara Novero[3], Milena Marsoni[1], Lorenzo Testa[1], Maria Concetta de Pinto[4], Angela Amoresano[2], Francesca Ortolani[1], Marcella Bracale[1] and Paola Bonfante[3]

[1]Department of Biotechnology and Life Science, Università dell'Insubria, via J.H. Dunant 3, I-21100 Varese, Italy; [2]Department of Chemical Sciences, Università di Napoli 'Federico II', via Cintia 4, I-80126 Napoli, Italy; [3]Department of Life Sciences and Systems Biology, Università di Torino, viale Mattioli 25, I-10125 Torino, Italy; [4]Department of Biology, Università di Bari 'Aldo Moro', via E. Orabona 4, I-70125 Bari, Italy

Authors for correspondence:
Paola Bonfante
Tel: +39 116705965
Email: paola.bonfante@unito.it

Marcella Bracale
Tel: +39 332421418
Email: marcella.bracale@uninsubria.it

Received: *15 December 2015*
Accepted: *12 January 2016*

New Phytologist (2016) **211:** 265–275
doi: 10.1111/nph.13895

Key words: antioxidant status, arbuscular mycorrhizal fungi (AMF), carbonylated proteins, endosymbiotic bacteria, plant host, proteome profiling.

Summary

- Arbuscular mycorrhizal fungi (AMF) are obligate plant biotrophs that may contain endobacteria in their cytoplasm. Genome sequencing of *Candidatus* Glomeribacter gigasporarum revealed a reduced genome and dependence on the fungal host.
- RNA-seq analysis of the AMF *Gigaspora margarita* in the presence and absence of the endobacterium indicated that endobacteria have an important role in the fungal pre-symbiotic phase by enhancing fungal bioenergetic capacity. To improve the understanding of fungal–endobacterial interactions, iTRAQ (isobaric tags for relative and absolute quantification) quantitative proteomics was used to identify differentially expressed proteins in *G. margarita* germinating spores with endobacteria (B+), without endobacteria in the cured line (B−) and after application of the synthetic strigolactone GR24.
- Proteomic, transcriptomic and biochemical data identified several fungal and bacterial proteins involved in interspecies interactions. Endobacteria influenced fungal growth, calcium signalling and metabolism. The greatest effects were on fungal primary metabolism and respiration, which was 50% higher in B+ than in B−. A shift towards pentose phosphate metabolism was detected in B−. Quantification of carbonylated proteins indicated that the B− line had higher oxidative stress levels, which were also observed in two host plants.
- This study shows that endobacteria generate a complex interdomain network that affects AMF and fungal–plant interactions.

Introduction

Many bacteria can replicate inside eukaryotic cells. This intracellular life style results in a wide range of interactions with their hosts (Toft & Andersson, 2010). Endobacteria have an impressive diversity in their genomic traits and can establish parasitic or mutualistic relationships with their host, which can deeply affect host cell function. Insect endosymbiosis is one of the best investigated examples of mutualism between endobacteria and animal cells: genomic sequencing of both partners has revealed functional compatibility that controls nutrient strategies and insect development (Wernegreen, 2012; Moran & Bennett, 2014).

Historically, observations of endobacteria inhabiting fungi were considered to be rare and primarily limited to some mycorrhizal and pathogenic fungi (Bonfante & Anca, 2009). However, extensive sequencing of environmental samples and detailed analysis of fungal genomes have indicated that these are not rare events. For example, a nitrogen-fixing bacterium was detected inside the pathogenic fungus *Ustilago* (Ruiz-Herrera *et al.*, 2015), the genomes of *Mollicutes*-related endobacteria (MRE) living inside many arbuscular mycorrhizal fungi (AMF) have been sequenced (Naito *et al.*, 2015; Torres-Cortés *et al.*, 2015), as has the genome of a betaproteobacterium living inside *Mortierella* (Fujimura *et al.*, 2014). The adaptation mechanisms involved in bacterial–fungal symbiosis have not been elucidated. To obtain insights into these interrelationships, we investigated the symbiotic relationship between *Candidatus* Glomeribacter gigasporarum (*Ca.* G. gigasporarum) and the AMF *Gigaspora margarita*. *Candidatus* G. gigasporarum is an obligate, stable and structurally integrated endosymbiont of *G. margarita*, which – on its part – forms symbiotic associations with roots of most land plants. This three-way interrelationship provides a very interesting example of a meta-organism (Bosch & McFall-Ngai, 2011).

The *Ca.* G. gigasporarum genome lacks some crucial metabolic pathways, indicating that the endobacteria are metabolically dependent on the fungal host for nutrients and energy (Ghignone

et al., 2012). This result explains why *Ca.* G. gigasporarum cannot be cultured outside of the host. This situation severely limits experimental efforts to define the molecular mechanisms underlying host–symbiont interactions. However, a *G. margarita* line was developed that lacks its endobacteria (designated as B− or cured line); this line is a stable wild-type (designated as B+ or wt line) variant that is still able to establish mycorrhizal symbiosis (Lumini *et al.*, 2007).

To understand the bacterial effect on fungal fitness, we used next-generation sequencing to analyse the transcriptional profile of *G. margarita* in the presence and absence of its endobacterium (Salvioli *et al.*, 2016). Transcriptional analysis was performed using germinated spores with and without GR24 treatment, which is a synthetic analogue of strigolactone (SL). SLs are plant hormones that play a key role in plant–fungal signalling (Al-Babili & Bouwmeester, 2015; Bonfante & Genre, 2015). In addition to the fungal sporification success, transcriptomic results indicate that the endobacterium affects a large number of fungal cell functions. In particular, it targets mitochondrial activity, upregulating the genes involved in respiration, ATP production and reactive oxygen species (ROS) detoxification.

Many studies have shown that mRNA levels only partially correlate with protein abundance (Maier *et al.*, 2009; Haider & Pal, 2013) as a result of translational and post-translational regulation. In mammalians, this is true for important regulators of cell development and differentiation (e.g. transcription factors and signalling proteins), whereas housekeeping proteins (e.g. ribosomal proteins, glycolytic proteins and tricarboxylic acid cycle proteins) show a better correlation with mRNA levels (Schwanhäusser *et al.*, 2011). Focusing on plant–microbe interactions, Feussner & Polle (2015) underlined how proteomics may increase the spatial resolution of RNA-based analyses, revealing, for example, basal immunity components. As a result of the technical challenges presented by our experimental system (neither AMF nor endobacteria can be cultivated or genetically transformed), we reasoned that the identification and quantification of the proteins expressed during the fungal–endobacterial interaction might provide a further level of understanding of our previous transcriptomic analysis (Salvioli *et al.*, 2016), providing a more realistic picture of gene function.

The aim of the present work was to analyse the proteomic profile of AMF *G. margarita* and its endobacterium, with and without GR24 treatment, in order to validate the hypothesis that proteomics may be closer to phenotype (Feussner & Polle, 2015) and may better explain some morphological traits of the cured line (Lumini *et al.*, 2007). A preliminary analysis of the proteomic profiles used classical two-dimensional gel electrophoresis (Salvioli *et al.*, 2010). We wanted to complement the previous study and improve the coverage of the protein changes associated with endosymbiosis. Therefore, we employed the alternative proteomic approach iTRAQ (isobaric tags for relative and absolute quantification). This non-gel-based technique enables the unbiased evaluation of protein expression in complex biological samples and has wide application in the biological and biomedical sciences (Cox & Mann, 2011). Data obtained via iTRAQ analysis were supported by transcriptomic and physiological analyses. The results provide new insights into the molecular mechanisms mediating endosymbiosis and into how bacteria provide direct and/or indirect ecological benefits, not only for their fungal host, but also for the plant. Indeed, the study shows that the endosymbiont can enhance the fungal response to endogenous ROS, increasing the total antioxidant activity of the fungus as well its glutathione content. This event can also influence the antioxidant status of mycorrhizal roots. This suggests the presence of a specific interdomain network involving the bacterial-mediated increase in fungal antioxidant capacity, which is subsequently transmitted to the mycorrhizal host plant.

Materials and Methods

Biological materials

Spores of *Gigaspora margarita* Becker and Hall (BEG 34, deposited at the European Bank of Glomeromycota) containing (B+) or not (B−) the *Ca.* G. gigasporarum endobacteria were used in this study. All the details concerning the propagation of B+ and B− spores, the protocol for spore germination, the treatment with the solution (10^{-7} M) of the synthetic SL analogue GR24 and the mycorrhization procedure are given in Salvioli *et al.* (2016). *Lotus japonicus* (Regel) K. Larsen seedlings were inoculated with the fungal spores using the 'Millipore sandwich' method (Novero *et al.*, 2002). Mycorrhizal status was checked after 4 wk. Mycorrhizal clover plants (*Trifolium pratense* L.) were maintained in pots containing sterilized quartz sand; roots were sampled after 3 months.

Protein extraction

Proteins were extracted from the four lines (B+, B+GR24, B−, B−GR24), starting from 500 spores for each one. Protein extractions from roots were performed, starting from 1 g of fresh material. Finely ground samples were suspended in 2.5 ml of extraction buffer (Tris-HCl, 0.5 M, pH 8; sucrose, 0.7 M; NaEDTA, 10 mM; ascorbic acid, 4 mM; β-mercaptoethanol, 0.4%; phenylmethylsulfonylfluoride (PMSF), 1 mM; leupeptin, 1 μM; pefabloc, 0.1 mg ml^{-1}). An equal volume of Tris-saturated phenol was added. The samples were mixed and incubated for 30 min at 4°C. The phenol phase was collected after 15 min of centrifugation at 5000 ***g*** at 4°C. Proteins were precipitated overnight with five volumes of ice-cold 0.1 M ammonium acetate in 100% methanol at −20°C. After 40 min of centrifugation at 17 000 ***g***, the protein pellet was washed twice in 0.1 M ammonium acetate and twice in ice-cold 80% acetone. The resulting pellets were dried and stored at −80°C until further processing. Three independent protein extractions were performed for each condition tested.

Protein digestion and iTRAQ labelling

An equal amount of spore proteins was prepared for each biological replication. Protein samples were reduced with 10 mM dithiothreitol (DTT), alkylated with 55 mM iodoacetamide,

digested using sequencing grade trypsin (Promega) at a ratio of 1 : 10 (w : w) for 12 h at 37°C, and labelled using an iTRAQ 4-plex kit (AB Sciex Inc., Framingham, MA, USA) according to the manufacturer's protocol. Samples were labelled with iTRAQ tags 114, 115, 116 and 117, respectively.

LC-MS/MS analysis

LC-MS/MS analysis was performed using an EASY-nLC capillary system (ThermoFisher Scientific, San Jose, CA, USA), coupled to an LTQ-Orbitrap XL hybrid mass spectrometer (ThermoFisher Scientific). Sample concentration and desalting were performed online using a column (180 μm × 20 mm; packed with 5-μm, 100-Å-pore-size Symmetry C18 material; ThermoFisher Corp.) at a flow rate of 15 μl min^{-1} for 1 min. Separation was accomplished on a capillary column (100 μm × 100 mm; packed with 1.7-μm, 130-Å-pore-size bridged ethyl hybrid [BEH] C18 material; ThermoFisher Corp.). A linear gradient of A and B buffers (buffer A, 3% acetone (ACN)–0.1% formic acid (FA); buffer B, 97% ACN–0.1% FA) from 7% to 45% buffer B over 124 min was used at a flow rate of 0.5 μl min^{-1} to elute peptides into the mass spectrometer. Columns were washed and re-equilibrated between LC-MS/MS experiments. Electrospray ionization was carried out at 1.7 kV, with the LTQ heated capillary set to 150°C.

Mass spectra were acquired in the Orbitrap in the positive-ion mode over the range of m/z 300–2000 at a resolution of 60 000. Mass accuracy after internal calibration was within 4 ppm. Simultaneously, tandem MS was acquired using the LTQ for the five most abundant, multiply charged species in the mass spectrum with signal intensities of > 8000 noise levels. MS/MS collision energies were set at 35%, using helium as the collision gas, and MS/MS spectra were acquired over a range of m/z values dependent on the precursor ion. Dynamic exclusion was set such that MS/MS for each species was acquired a maximum of twice. All spectra were recorded in profile mode for further processing and analysis. Xcalibur (ThermoFisher Corp.) software was used for MS and MS/MS data analysis.

iTRAQ protein identification and quantification

For protein identification, MS/MS data were searched using in-house Mascot v.2.3.02 (Matrix Science, London, UK) against the 'Fungi' and 'Bacteria' subsets of the National Center for Biotechnology Information (NCBI). The search parameters were as follows: threshold set-off at 0.05 in the ion-score cut-off (with 95% confidence); MS/MS fragment ion mass tolerance of ± 0.6 Da; enzyme specificity was set to trypsin with one missed cleavage; peptide tolerance was set at 10 ppm; fixed modifications of carbamidomethylation at cysteine (Cys) and iTRAQ 4plex at lysine (Lys) and the N-terminal amino group of peptides; variable modifications of oxidation at methionine and glutamine as pyroglutamic acid; charge states of peptides were set to + 2 and + 3. Only peptides with significance scores greater than 'identity_score' were counted as identified. Mascot analysed three biological replicates of the iTRAQ data; only data with a false discovery rate (FDR) < 5% were used for subsequent data analysis.

To demonstrate repeatability, the protein abundances between various biological replicates were compared and the ratios for the proteins in each comparison were compared with unity. The difference was plotted against the percentage of the proteins quantified. For quantitative changes, a 1.2-fold cut-off was set to determine the up-accumulated and down-accumulated proteins, with $P < 0.05$ present in at least two replicates. Quantitative analysis was performed with Scaffold v.3.0 (http://www.proteomesoftware.com).

A comparison between *Rhizophagus irregularis* and *G. margarita* transcriptomes has revealed that, notwithstanding their deep differences in phylogeny, life cycle and ecological strategies, both AM fungi have a strict genetic relatedness (Salvioli *et al.*, 2016). According to this and in the absence of a reference proteome, the identified *G. margarita* proteins were blasted against the NCBI database for *R. irregularis* (E-value < e^{-40}, identity ≥ 40%). The proteins identified as bacterial proteins were blasted against the NCBI database of *Ca.* G. gigasporarum (E-value < e^{-40}, identity ≥ 40%).

For Venn diagrams, we used the open source program Venny 2 (J. C. Oliveros (2007–2015) Venny. An interactive tool for comparing lists with Venn's diagrams. http://bioinfogp.cnb.csic.es/tools/venny/index.html).

Respiratory activity

O_2 consumption was measured using a Clark-type electrode (Hansatech Ltd., Hardwick Industrial, Norfolk, UK) calibrated between 0% and 100% with atmospheric oxygen. The respiration chamber was connected to a water circulator to maintain a constant temperature of 30°C. The reaction was carried out at a constant stirrer speed in a chamber volume of 1 ml. The recording of oxygen consumption was started by adding 1 ml of distilled H_2O into the chamber, followed by 100 fungal spores. Spores were germinated for 3 d at 30°C in the dark. For GR24 treatment, the spores were incubated for 3 h with 10^{-7} M of GR24 before polarographic measurement. O_2 consumptions were read for 15 min. An increase in O_2 consumption in spores was calculated by comparison of the slope with distilled water in equilibrium with the O_2 atmosphere (control).

H_2O_2, glutathione and total antioxidant activity

After 3 d of germination, 2700 spores of each line were collected by filtration on Whatman 3MM paper and separately weighed for the determination of H_2O_2, total antioxidant activity and total glutathione. For total antioxidant activity and total glutathione, 0.1 g of spores were ground in a mortar in liquid nitrogen with 10 volumes of acidified methanol and 5% metaphosphoric acid, respectively. After centrifugation at 20 000 ***g***, the levels of total antioxidant activity and total glutathione were measured in the supernatants according to Locato *et al.* (2008).

For intracellular H_2O_2 determination, 0.1 g of spores were homogenized with 10 volumes of ice-cold 5% trichloroacetic acid. The extracts were centrifuged for 20 min at 1400 ***g***, and the supernatant was neutralized in the presence of 0.1 M phosphate buffer (pH 7.0) with 2 M KOH to *c.* pH 7.0. H_2O_2 was measured in the extract through the oxidation of 3,3′,5,5′-tetramethylbenzidine in the presence of peroxidase according to Sgobba *et al.* (2015).

Detection of carbonylated proteins in fungal and plant hosts

The proteins were extracted as described above; 20 μg of proteins were derivatized with 2,4-dinitrophenylhydrazine (DNPH), as described previously with some modifications (Levine *et al.*, 1994). Briefly, the proteins were denatured, adding sodium dodecylsulfate (SDS) at a final concentration of 6%. The derivatization was performed by adding 1 volume of 10 mM DNPH in 2 M HCl. Only 2 M HCl was added to the negative control. After 30 min of incubation at room temperature, the mixture was neutralized by adding 1 volume of neutralization solution (2 M Tris, 30% glycerol). Proteins were separated by 12% SDS-PAGE and transferred to polyvinylpyrrolidone (PVP) membrane (Serva Electrophoresis GmbH, Heidelberg, Germany). The oxidatively modified proteins were detected using anti-DNPH antibodies (anti-dinitrophenyl-group antibodies; Sigma, USA) and visualized by a chemiluminescence detection kit (SuperSignal, Pierce Biotechnology, Rockford, IL, USA). Colloidal Coomassie Brilliant Blue (CCBB) was used to stain a duplicate gel. Alternatively, after electrophoresis, the proteins were stained with Bio-Safe Coomassie (Bio-Rad) and then processed for immunoblotting. Gel and immunoblot images were acquired using GS-800 (Bio-Rad) and analysed using ImageJ software (http://imagej.nih.gov/ij/).

Real-time PCR assays

For reverse transcription-quantitative polymerase chain reaction (RT-qPCR) validation, total RNA was extracted from batches of 100 *G. margarita* spores with an Rneasy Plant Mini Kit (Qiagen, Hilden, Germany) and treated with a Turbo DNA-free kit (Life Technologies, Carlsbad, CA, USA). The samples were then reverse transcribed using Superscript II Reverse Transcriptase (Life Technologies). Quantitative real-time PCR experiments and data analysis were carried out as described in Salvioli *et al.* (2012), using as a reference gene for transcript normalization the *G. margarita* translation elongation factor (EF1-α). The primer names and corresponding sequences are listed in Supporting Information Table S1.

Results and Discussion

A total soluble proteomic dataset from the AMF *G. margarita* was generated using iTRAQ analysis under the following four conditions: *G. margarita* B+ (wild-type) or B− (cured) germinating spores, treated with or without 10^{-7} M of GR24. Each of the four samples (B+, B−, B+GR24 and B−GR24) was labelled with one of four reagents of the iTRAQ four-plex, and samples were combined into one aliquot. Triplicate labelling was performed, which showed a high level of reproducibility (data not shown). Data from the three replicates were merged and used for protein identification. Mascot analysis detected FDR < 5%. For the second step, protein profile changes in the four samples were analysed by Scaffold software and used to generate a proteomic dataset consisting of 156 fungal proteins (Table S2; Fig. S1a). This approach complements the genome data and protein prediction analysis of *R. irregularis*, and provides a novel platform for the investigation of AMF function (Recorbet *et al.*, 2013; Tisserant *et al.*, 2013; Lin *et al.*, 2014).

Candidatus G. gigasporarum affects a core set of fungal proteins

The proteomes of B+ and B− lines were analysed after 7 d of germination. We quantified and identified 127 unique fungal proteins. Statistical analysis indicated that 61 proteins differed in the two lines: the levels of 26 proteins were higher and those of 35 proteins were lower in B− than in B+. These differentially expressed proteins are shown in Table S3 and Fig. S1(b). The proteins were annotated into 10 functional categories based on gene ontology, Blast alignment and information in the literature. The most abundant classes were 'metabolic processes' (33%), 'protein synthesis and degradation' (16%) and 'unknown function' (24%).

When we compared the two germinating spore proteomes of B−GR24 and B+GR24, a total of 89 proteins were quantified and identified. Statistical analysis indicated that 49 proteins differed in the two lines: the levels of 26 proteins were higher and those of 23 proteins were lower in B−GR24 than in B+GR24. These differentially expressed proteins are shown in Table S4 and Fig. S1b. The proteins were classified into seven functional categories based on gene ontology, Blast alignment and information in the literature. The most abundant classes were 'metabolic processes' (27%), 'protein folding' (20%), 'protein synthesis and degradation' (18%) and 'unknown function' (18%). Among the 49 differentially expressed proteins in these two samples, 19 overlapped with the 61 proteins previously identified as differentially expressed in the B+ and B− proteomes. We conclude that these 19 proteins (listed in bold in Tables S3 and S4) are good candidates for involvement in specific fungal responses to the endobacterium.

The combined results indicate that endobacteria modulate fungal protein expression and metabolism in the presence/absence of SL, and identify some of the primary molecular determinants involved in host adaptation responses (discussed in the subsequent section). Our analysis also detected and identified 24 bacterial proteins in the B+ and B+GR24 fungal proteomes. Of these, the levels of eight proteins were higher and nine were lower after GR24 treatment, indicating that SLs affect endobacteria (Table S5). However, only five of these 17 proteins found a direct match using Blast analysis in the *Ca.* G. gigasporarum genome (Ghignone *et al.*, 2012); four of these five proteins were directly attributable to *Ca.* G. gigasporarum, and expression levels were

modulated by SL. These proteins might function in extracellular bacterial communication. One was an outer membrane protein containing a YadA domain; the trimeric autotransporter adhesin YadA is considered to be one of the most important virulence factors in *Yersinia enterocolitica* (Pepe *et al.*, 1995). Current models suggest that YadA mediates *Yersinia* adhesion to host cells, thus facilitating the injection of effectors via the type III secretion system (T3SS) (Keller *et al.*, 2015; Mühlenkamp *et al.*, 2015). It is tempting to fit this model to the *Ca.* G. gigasporarum–fungal interaction because endobacterial genes encoding T3SS components display specific expression patterns throughout the different stages of the fungal life cycle (Ghignone *et al.*, 2012). The outer membrane protein belonging to the OmpA/MotB family is required for pathogenesis and host interactions in *Escherichia coli* (Selvaraj *et al.*, 2007), and accumulates in response to GR24 treatment. Two other endobacterial proteins possessing interesting features are influenced by SL treatment: the osmotically inducible protein OsmY, which is a periplasmic sensory protein that confers stress resistance (e.g. low phosphate conditions) to *Salmonella* when living in macrophage vesicles (Zheng *et al.*, 2015), and a protein with unknown function belonging to the ElaB family of membrane-anchored, ribosome-binding proteins.

In summary, these proteomic data provide experimental evidence for the hypothesis that endobacteria communicate with fungal hosts via membrane proteins, such as the T3SS (Ghignone *et al.*, 2012), and those involved in sensing nutrient concentration. The data also suggest that plant signals are directly or indirectly perceived by endobacteria (Anca *et al.*, 2009).

Candidatus G. gigasporarum affects proteins involved in fungal growth, morphology and calcium signalling

Germinating spores of B+ and B+GR24 accumulated proteins involved in DNA replication, transcription and protein synthesis (Tables S3, S4), suggesting that endobacteria enhance fungal growth. This result is consistent with the higher growth rate of the B+ line than the B− line (Lumini *et al.*, 2007). One of the most strongly differentially expressed proteins was a Rho-GDP-dissociation inhibitor (Rho-GDI), which was downregulated in the B− and B−GR24 proteomes. The *Rho-GDI* transcript (comp37206_c0_seq1) level was also lower in the B− line (Salvioli *et al.*, 2016). Rho-GDI represses monomeric Rho-GTPases, which control many fundamental cellular processes, such as cytoskeletal organization, vesicle trafficking and bud site selection (DerMardirossian & Bokoch, 2005). Curing the colonial marine bryozoan *Bugula neritina* from its endosymbiont *Candidatus* Endobugula sertula also resulted in Rho-GDI downregulation and disrupted cytoskeletal organization (Mathew & Lopanik, 2014). Curing *G. margarita* from its endobacterium caused phenotypic changes in the cell wall, lipid drops and cytoplasmic viscoelasticity (Lumini *et al.*, 2007). The B− line has a denser and more extensively aggregated cytoplasm than that in the B+ line; this could be a result of Rho-GDI downregulation and the accumulation of actin and tubulin proteins (Tables S3, S4).

It is interesting to note that the Pmt6 protein mannosyltransferase accumulated in the B− cured line. Pmt proteins initiate *O*-glycosylation of secreted fungal proteins and are involved in fungal cell wall rigidity. *Candida albicans* mutants lacking one or two *Pmt6* alleles grow normally, but exhibit morphogenetic defects, indicating that Pmt6 regulates secreted proteins that are involved in morphogenesis (Timpel *et al.*, 2000). Being involved in cell wall metabolism and cytoplasm viscoelasticity, these proteins offer a mechanistic explanation for the thick, rigid cell wall and dense cytoplasm observed in the cured fungi (Lumini *et al.*, 2007).

The vacuolar calcium-transporting ATPase PMC1 strongly accumulated in the B− line treated with GR24. In plant and yeast cells, the vacuole serves as the principal site of Ca^{2+} sequestration and contains 95% of total cellular Ca^{2+} stores (Cunningham, 2011). Deletion of *PMC1* in yeast effectively reduces cell growth in high-Ca^{2+} environments, suggesting that PMC1 plays a significant role in vacuolar Ca^{2+} sequestration. Elevations in cytosolic Ca^{2+} increase *PMC1* expression (Cunningham & Fink, 1996). Many fungal genes related to Ca^{2+} homeostasis and signalling have been identified in the *Glomus intraradices* genome (Liu *et al.*, 2013), and their transcripts are differentially regulated. This is consistent with our proteomic data. Transcripts of these same genes and the putative Ca^{2+}-transporting ATPase were also detected in the *G. margarita* transcriptome (Salvioli *et al.*, 2016). These transcripts were slightly upregulated in the GR24-treated B− line. Higher cytosolic Ca^{2+} levels have been detected in germinating spores of the cured line (Salvioli *et al.*, 2016) using a cell-permeant aequorin peptide (Moscatiello *et al.*, 2014), and SL treatment further enhances cytosolic Ca^{2+} concentrations in the cured line.

In summary, PMC1 upregulation in the GR24-treated B− line suggests that Ca^{2+} homeostasis changes in fungi cured of the endobacterium. *Candidatus* G. gigasporarum might act as a specific calcium store; in its absence, calcium accumulates in the cytoplasm and in the vacuole. Therefore, the observed reduction in ATP content in the cured line could also be explained by ATP consumption required by PMC1 to store calcium inside the vacuole and by the negative interference of cytoplasmic calcium on ATP production (Case *et al.*, 2007).

Curing *G. margarita* of its endobacterium induces a metabolic shift towards alternative reducing pathways

Approximately 33% of the differentially expressed proteins in B+ and B− lines were involved in metabolic processes (Table S3). Proteins that are differentially expressed in the B+ line include a subunit of NADH-ubiquinone reductase, which is involved in mitochondrial oxidative phosphorylation; the mitochondrial malate dehydrogenase (MDH1), which converts malate to oxaloacetate in the tricarboxylic acid cycle; and triose phosphate isomerase (TPI). These results are supported by transcriptomic data indicating that genes involved in oxidative phosphorylation are upregulated and ATP production increases in the B+ line, which suggests that endobacteria increase the bioenergetic potential of host fungi (Salvioli *et al.*, 2016). To obtain evidence for this hypothesis, we measured fungal respiration in the B+ and B− lines. Polarography was sufficiently sensitive to detect the O_2 consumption rate in 100 *G. margarita* spores after 3 d of

germination. The results showed that O_2 consumption was *c.* 50% higher in the B+ line than in the B− line. As expected, GR24 treatment for 3 h increased O_2 consumption for both lines, but the respiratory capacity in the B+ line was *c.* 50% higher than that in the B− line (Table 1).

These results raised the question of what metabolic pathways are used for energy production in the cured *G. margarita* line, as energy demands are crucial during plant colonization. Proteomic analysis provided some insight into an alternative reducing pathway in the cured line. The following two proteins upregulated in the B− line were involved in the pentose phosphate pathway (PPP): the phosphogluconate dehydrogenase (decarboxylating enzyme) GND2 and the D-glyceraldehyde-3-phosphate transaldolase TAL1. These proteins operate during oxidative and non-oxidative phases of the PPP. This central pathway produces reduced equivalents in the form of NADPH during the oxidative PPP phase, and produces precursors for nucleic acid and aromatic amino acid biosynthesis during the non-oxidative PPP phase. Ralser *et al.* (2007) showed that dynamic re-routing of metabolic flux to the PPP, with concomitant NADPH generation, was a conserved response to oxidative stress. NADPH provides the reducing potential for most antioxidant and regulatory enzymes controlling cellular redox homeostasis.

Another NADPH source in the cured line is NADP+-dependent isocitrate dehydrogenase (IDP1). This enzyme has been studied in *Saccharomyces cerevisiae*, where it catalyses the conversion of D-*threo*-isocitrate to 2-oxoglutarate in mitochondria. IDP has also been localized to the cytosol (IDP2) and peroxisome (IDP3). These three IDPs are involved in defence against oxidative stress in yeast (Minard & McAlister-Henn, 2001; Contreras-Shannon & McAlister-Henn, 2004). In the current study, IDP differentially accumulated in the cured line, as confirmed by transcriptional results (Fig. 1), suggesting that the B− line had defective regulation of oxidative status.

GR24 treatment induced the expression of some proteins involved in maintaining the cellular redox balance in the B− line, including a cytosolic aldehyde dehydrogenase (ALDH), an alcohol dehydrogenase (ADH) and a cytosolic glycerol-3-phosphate dehydrogenase (GPD). RT-qPCR analyses confirmed the differential expression of *ALDH* and *GPD* transcripts in the B+ and B− lines, whereas changes in ADH transcript levels were not detected (Fig. 1). Cytosolic ALDH oxidizes acetaldehyde to acetic acid and produces NADPH. The ability to act as an aldehyde scavenger during lipid peroxidation is another universal ALDH function found across species. Upregulation of ALDH is a stress response in bacteria, plants, yeasts and mammals (Singh *et al.*, 2013). ADH and GPD are reported to maintain redox balance in *S. cerevisiae* under limited respiratory capacity. Under aerobic conditions, oxidation of NADH produced during glycolysis occurs via the respiratory chain, which transfers the reducing equivalents to oxygen. Under limited respiratory capacity, *S. cerevisiae* strongly increases alcohol fermentation and glycerol production via GPD to accommodate non-respiratory oxidation of NADH to NAD+ (Valadi *et al.*, 2004; Snoek & Steensma, 2007). In light of the current study, it appears that the cured line may have a deficit in reducing power and greater oxidative stress; consequently, this line specifically upregulates proteins in alternative pathways that can remediate the redox balance (Fig. 2). Interestingly, substantial modifications in the energy metabolic pathways have already been reported to occur as a consequence of symbiosis establishment, as in the nitrogen-fixing *Rhizobium*–legume association (Karunakaran *et al.*, 2009).

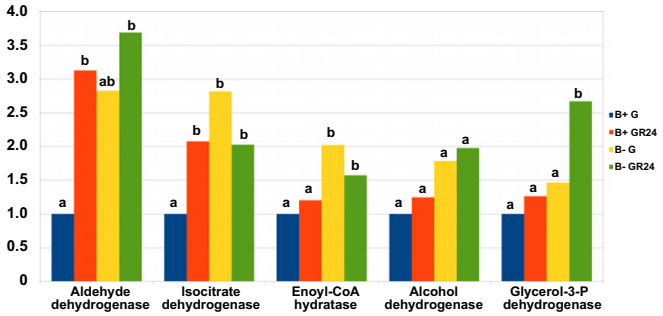

Fig. 1 Relative quantification of gene expression obtained for a subset of metabolism-related sequences. Expression data were obtained for *Gigaspora margarita* B+ germinating spores (B+), B− germinating spores (B−), B+ strigolactone-treated spores (B+GR24) and B− strigolactone-treated spores (B−GR24). For each transcript, fold changes were calculated considering B+ as the reference basal condition (for the latter, the fold change = 1). Statistically supported differences are indicated with different letters according to a Kruskal–Wallis non-parametric test at $P < 0.05$.

Table 1 O_2 consumption in *Gigaspora margarita* lines

	Slope values			
Experiments	B+	B−	B+GR24	B−GR24
1	0.9	0.4	0.83	0.5
2	1.1	0.4	0.85	0.5
3	0.65	0.42	0.9	0.5
4	0.7	0.4	1.2	0.4
Mean	0.84	0.40[a,b]	0.95	0.48[a,b]
Standard deviation	0.2	0.01	0.17	0.05

Relative differences in O_2 consumption were measured by polarography in spores germinated for 3 d and treated for 3 h with or without GR24.
[a]Values significantly different from B+ (*t*-test, $P < 0.01$).
[b]Values significantly different from B+GR24 (*t*-test, $P < 0.01$).

Lipid catabolism provides an important energy resource for AMF

Another important change in fungal basal metabolism in the B+ and B− lines involves lipid catabolism. Lipid metabolism in AMF has been extensively studied. Although lipids are the most important energy storage form, the *R. irregularis* genome does not contain any gene involved in *de novo* fatty acid synthesis (Tisserant *et al.*, 2013; Wewer *et al.*, 2014). Gluconeogenesis, which catabolizes lipids into hexoses, has been reported in the AMF extraradical mycelium (Pfeffer *et al.*, 1999), and has been confirmed for *R. irregularis* (Wewer *et al.*, 2014) and our *G. margarita* isolates. One of the key enzymes of the fatty acid β-oxidation pathway, the enoyl-CoA hydratase FOX2, was

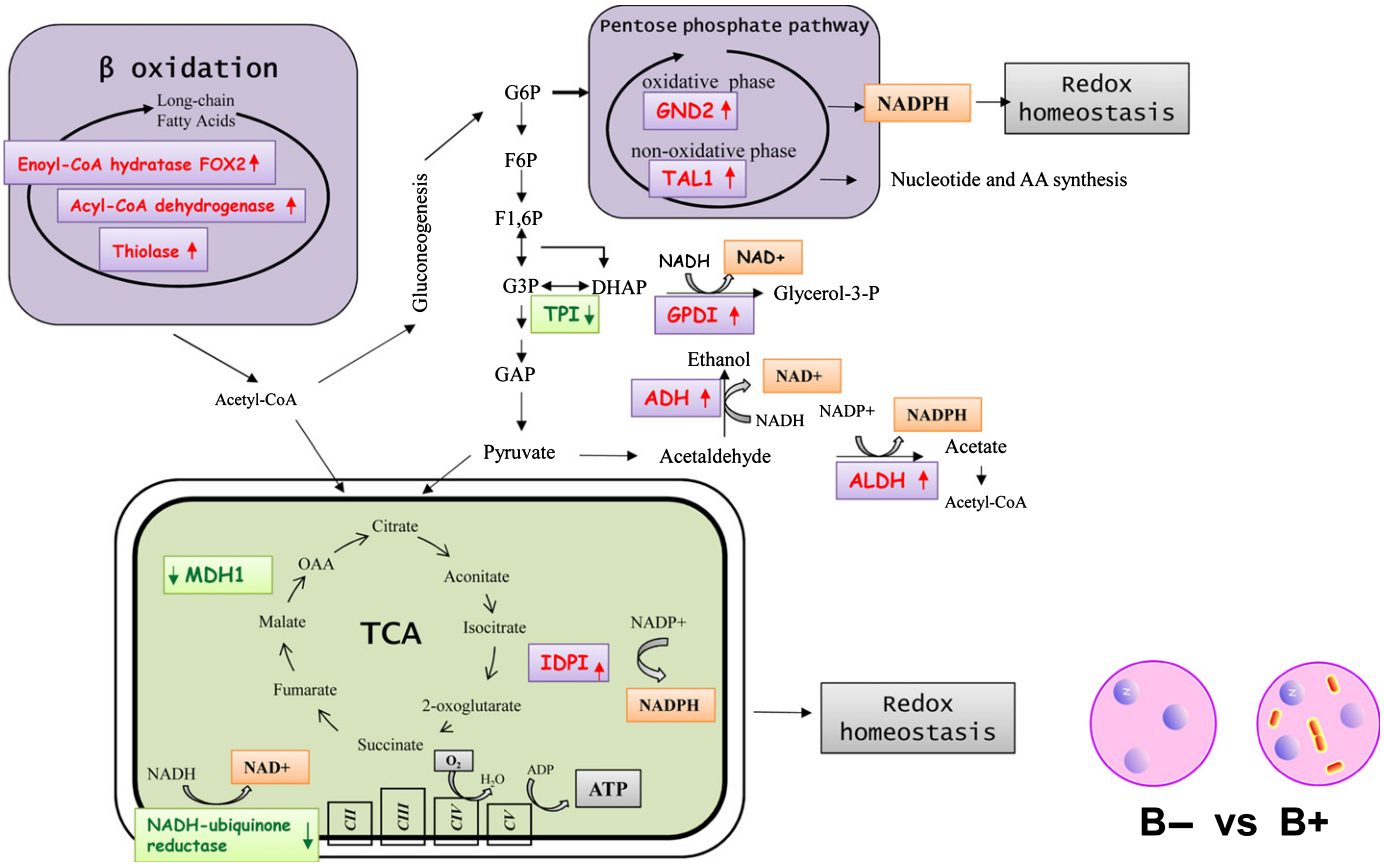

Fig. 2 Schematic overview of metabolic pathways differentially regulated in the *Gigaspora margarita* B– line in comparison with the B+ line on the basis of the proteins identified in the current study. Proteins that were upregulated are indicated in red; those that were downregulated are indicated in green. AA, amino acid; ADH, alcohol dehydrogenase; ALDH, aldehyde dehydrogenase; DHAP, dihydroxyacetone phosphate; F1,6P, fructose-1,6-diphosphate; F6P, fructose-6-phosphate; G6P, glucose-6-phosphate; GAP, glyceraldehyde-3-phosphate; GND2, phosphogluconate dehydrogenase; GPD, glycerol-3-phosphate dehydrogenase; IDP1, $NADP^+$-dependent isocitrate dehydrogenase; MDH1, malate dehydrogenase; OAA, oxalacetic acid; TAL, transaldolase; TCA, tricarboxylic acid; TPI, triose phosphate isomerase.

upregulated in the B– line compared with that in the B+ line, also after GR24 treatment. This result was confirmed by RT-qPCR analysis (Fig. 1). In the GR24-treated B– line, we also detected higher levels of one thiolase and one acyl-CoA dehydrogenase, which are involved in the β-oxidation pathway. Therefore, catabolism of fatty acids into hexoses appears to increase in the cured line. This was further supported by the accumulation in the B+ line of a WD repeat-containing protein homologue to the glucose-induced degradation complex subunit GID7 of *R. irregularis*. GID7 is involved in proteasomal degradation of fructose-1,6-bisphosphatase (FBPase), which is a key regulatory enzyme of gluconeogenesis. FBPase is degraded via the ubiquitin proteasome system when cells are replenished with glucose (Regelmann *et al.*, 2003). In fungi, FOX2 is repressed by glucose (Ebbole, 1998). The observed change in lipid catabolism could also be associated with higher bioenergetic potential in the B+ line as a result of the upregulation of oxidative phosphorylation. Our proteomic and genetic evidence for increased β-oxidation in the B– line is consistent with other morphological and biochemical studies showing that cured spores have reduced lipid storage (Lumini *et al.*, 2007; Salvioli *et al.*, 2010).

Endobacteria elicit fungal antioxidative activity, which is subsequently transmitted to mycorrhizal host plants

Transcriptomic results suggested that higher respiration was associated with greater ROS detoxification in the B+ line (Salvioli *et al.*, 2016). Our proteomic data identified proteins that could be involved in this process. The peroxiredoxin (Prx) Tsa1, which is the most abundant Prx in yeast, accumulated in the B+ line and in the GR24-treated B+ line. This result was confirmed by transcriptomic analysis of the GR24-treated B+ line (data not shown). Tsa1 is crucial for resistance to ROS, and is required during normal aerobic growth conditions (Iraqui *et al.*, 2009). Tsa1 protects cells against oxidative stress caused by misfolding and aggregation of nascent proteins. Protein aggregation is accompanied by mitochondrial fragmentation, and Tsa1 localizes to sites of protein aggregation. Disruption of mitochondrial function rescues the ROS sensitivity of *tsa1* mutants (Weids & Grant, 2014). Tsa1 accumulation in the B+ line reflects the need to remove excess ROS generated during respiration. ROS detoxification processes were also activated in the B– line as a result of the induction of cysteine Prx and glutathione-S-transferase (GST). GR24 treatment further stimulates ROS detoxification in

the B+ line and induces the accumulation of Tsa1, GST and a copper- and zinc-containing superoxide dismutase (Cu/Zn-SOD). Treatment of *G. margarita* with root exudate has been reported to induce Cu/Zn-SOD (Lanfranco *et al.*, 2005).

Transcriptomics and proteomics data indicated that *G. margarita* exhibited different responses to ROS depending on whether *Ca.* G. gigasporarum was present or absent. We tested the hypothesis that endobacteria promote fungal responses to oxidative stress. The total antioxidant activities of the soluble extracts were analysed separately in the B+ and B− spores. The total antioxidant activity was lower in B− (Table 2). Among the hydrophilic antioxidants, attention was focused on the change in the level of GSH. The fungus without endobacteria had 43% of total GSH content (reduced plus oxidized forms), lower than that of the B+ line (Table 2). Moreover, to obtain a direct measurement of cellular ROS, we analysed the H_2O_2 concentration in both systems. In B−, the H_2O_2 content was 30% higher than that of B+. However, the very low concentrations measured do not allow statistically significant results to be obtained.

Oxidative damage can occur when there is an imbalance between ROS production and antioxidant defence. Therefore, we examined the accumulation of oxidatively modified polypeptides by performing immunoblot analysis of carbonylated proteins. Protein carbonylation is one of the most harmful and irreversible oxidative protein modifications, and is considered as a major hallmark of oxidative damage (Fedorova *et al.*, 2014). The protein carbonylation level was higher in the B− line than in the B+ line, indicating that the absence of endobacteria leads to a higher level of oxidative damage (Fig. 3). Surprisingly, we also detected a significant increase in protein carbonylation levels in the GR24-treated B+ line (Fig. 3). This suggests that there is an increased imbalance between ROS levels and the capacity of antioxidant scavengers as a result of GR24-mediated stimulation of respiration, or that SLs are perceived by AMF as xenobiotics that may cause transient oxidative damage (Salvioli *et al.*, 2016). However, with this exception, the results support the hypothesis that redox homeostasis is disrupted in the cured fungal line under constitutive conditions.

The key question arising from this study is whether the higher antioxidant capacity of the B+ line helps the host plant cells to maintain cellular redox homeostasis during the symbiosis. To answer this question, we compared the protein carbonylation profiles of clover roots after mycorrhizal colonization with the B+ (B+Myc) or B− (B−Myc) lines. The levels of oxidatively modified proteins were higher in roots colonized by the B− line (Fig. 4). This result was confirmed in a parallel experiment testing *Lotus japonicus* roots colonized by the B+ or B− lines (Fig. S2).

Table 2 Intracellular levels of H_2O_2, total antioxidant activity (TAA) and total glutathione (GSH) in *Gigaspora margarita* lines

	H_2O_2 (nmol g^{-1} FW)	TAA (nmol Trolox eq g^{-1} FW)	GSH (nmol g^{-1} FW)
B+	6.1 ± 0.6	884 ± 35	189 ± 14
B−	8.5 ± 0.4	543 ± 30[a]	107 ± 11[a]

The values are the mean ± SE of three independent experiments.
[a]Values significantly different from B+ (*t*-test, $P < 0.05$).

To understand whether the carbonylated proteins detected in the mycorrhizal roots were of plant or fungal origin, proteins were submitted to carbonylation analysis after two-dimensional separation (2DE). Among the differentially carbonylated proteins, we randomly selected and identified seven by MS/MS (Methods S1; Fig. S3). All the selected proteins corresponded to *Medicago truncatula* proteins (Table S6); they exhibited at least one peptide with oxidized methionine residues. Putting together these results and data from the transcriptomic analysis of mycorrhizal roots, revealing that only a small number of fungal transcripts (2.5%) are detectable (Ruzicka *et al.*, 2013), we may conclude that the carbonylated proteins detected in the mycorrhizal roots are mostly of plant origin.

Overall, the results indicate that endobacteria may affect the host plant through the intermediary of an AM fungus. The enhanced detoxification of ROS and resistance to oxidative stress may help plant roots to adapt to complex soil environments characterized by strong fluctuations in abiotic and biotic parameters.

Conclusions

Endobacterial symbionts of insects, invertebrates and vertebrates are excellent models for the investigation of the molecular links between bacteria, bacterial metabolites and host physiologies (Lee & Hase, 2014). Bacteria and endobacteria also associate with fungi, as either extracellular microbes (Frey-Klett *et al.*, 2011) or endobacteria in symbiotic and pathogenic fungi (Bonfante, 2014; Ruiz-Herrera *et al.*, 2015). Previous research efforts have focused on the identification of endobacteria rather than on defining the mechanisms that regulate the symbiotic interactions. The molecular relationships among fungal endobacteria, bacterial metabolites, fungal signalling pathways and fungal physiology are largely unknown. An exception is the *Rhizopus* system; *Rhizopus* hosts the endobacterium *Burkholderia rhizoxinica*, which produces a deleterious phytotoxin affecting the infected plant (Lackner & Hertweck, 2011).

In this study, we examined the relationship between the mycorrhizal fungus *G. margarita* and its obligate endobacterium *Ca.* G. gigasporarum. This symbiotic relationship appears to be stable and has been evolutionarily maintained for 400 million yr (Mondo *et al.*, 2012). We used a combination of proteomic, physiological, molecular and cellular approaches to conclusively demonstrate that the endobacterium affects fungal growth and development via its effects on lipid catabolism, cell wall organization and cytoplasmic characteristics. Proteomic analysis indicated that the endobacterium promoted fungal oxidative phosphorylation and increased respiratory activity. By contrast, fungi cured of the endobacterium exhibited metabolic shifts favouring PPP as an alternative method to acquire reducing power. These results are consistent with those for another group of mycorrhizal fungi, the ericoid fungi, which were subjected to heavy metal stress (Chiapello *et al.*, 2015). Our results using cured fungi clearly demonstrate that the endobacterium is crucial for optimum fungal cell homeostasis.

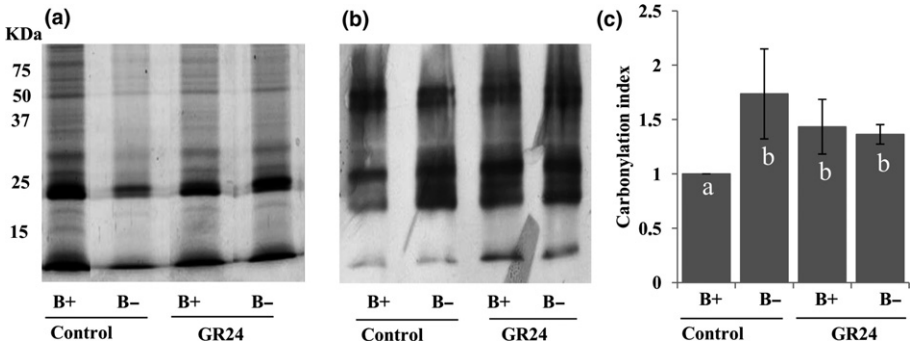

Fig. 3 Protein carbonylation profiles of *Gigaspora margarita* B+ and B− lines without and with GR24 treatment: (a) protein stain, (b) anti-DNP (2,4-dinitrophenol) immunoassay, (c) relative protein carbonylation values (referred to the B+ sample) expressed as the carbonylation index, after normalization for protein amounts. Data (means ± SD, $n = 3$) were subjected to one-way analysis of variance (ANOVA). Bars not accompanied by the same letter are significantly different at the 5% level using Tukey's test.

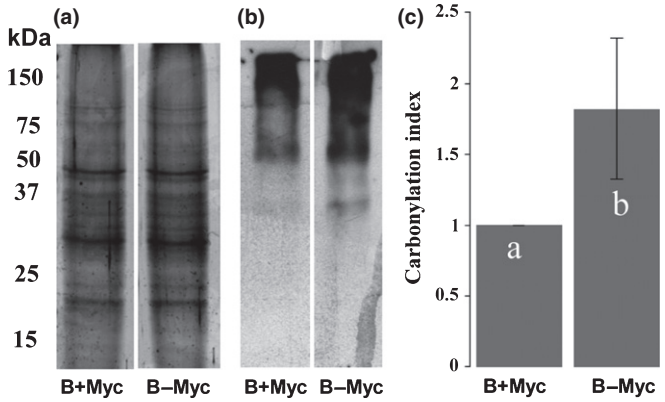

Fig. 4 Protein carbonylation profiles of clover roots after mycorrhizal colonization with B+ or B− lines: (a) protein stain, (b) anti-DNP (2,4-dinitrophenol) immunoassay, (c) relative protein carbonylation values (referred to the B+ sample) expressed as the carbonylation index, after normalization for protein amounts. Data (means ± SD, $n = 3$) were subjected to one-way analysis of variance (ANOVA). Bars not accompanied by the same letter are significantly different at the 5% level using Tukey's test.

The second novel result of our investigation is that curing the fungi of its endobacteria induced increased oxidative stress, which was also subsequently transmitted to the third partner of the system: the host plant. Carbonylated proteins are considered to be specific markers of oxidative stress, and have been identified in many plant species at different stages of growth and development (Debska *et al.*, 2012). This suggests that protein carbonylation may be involved in cellular signalling. Recent work has reported a link between ROS-based protein carbonylation and reactive nitrogen species (RNS)-based protein nitrosylation (Lounifi *et al.*, 2013). Our data open up the way to investigate redox proteomics in mycorrhizal plants. Recent studies have reported that ROS-related pathways are important for both pathogenic and symbiotic plant–fungal interactions (Samalova *et al.*, 2014), but the molecular mechanisms regulating these interactions are largely unknown.

In conclusion, this study has shown that the presence or absence of an endobacterium in a colonizing AMF can modulate the redox status of a host plant root system. This could be the indirect result of the AM symbiosis established by the cured fungal line: even if the latter does not cause a clear mycorrhizal phenotype, it has some growth defect (Lumini *et al.*, 2007), and the symbiotic functionality in terms of phosphate content is negatively impacted (Salvioli *et al.*, 2016). These results raise new questions about interspecies molecular interactions that occur under field conditions when the whole plant interacts with highly diverse microbiota (Bulgarelli *et al.*, 2013). The biodiversity of plant microbiota has been the subject of many studies, but limited attention has been given to plant responses.

Acknowledgements

The authors express their thanks to: Stefano Ghignone and Francesco Venice for bioinformatics support; Antonella Faccio for electron microscopy observations; Maria Teresa Della Beffa and Sara Torrielli (University of Torino) for taking care of spore production; Alberto Vianelli and Simone Barera (Insubria University) for their very helpful support with polarographic measurements; and the Functional Genomics Center Zürich (FGCZ) for highly valuable technical support. This research was funded by the Ateneo Project (ex 60%) to P.B. A.S.'s fellowship was granted by the Piedmont Region and University of Torino. F.O. is a student of the PhD School in 'Biotechnology Life Sciences and Surgical Technologies' at Insubria University.

Author contributions

C.V., A.C., M.M., F.O. and L.T. developed the proteomic dataset; M.C.deP. and C.V. performed the biochemical and physiological experiments; A.S. performed the transcriptomic experiments; M.N. developed the biological material; C.V., A.S., M.N., A.A., M.B. and P.B. analysed the data; C.V., M.B. and P.B. wrote the manuscript; M.B. and P.B. designed the experiments and supervised the research.

References

Al-Babili S, Bouwmeester HJ. 2015. Strigolactones, a novel carotenoid-derived plant hormone. *Annual Review of Plant Biology* **66**: 161–186.

Anca IA, Lumini E, Ghignone S, Salvioli A, Bianciotto V, Bonfante P. 2009. The ftsZ gene of the endocellular bacterium '*Candidatus* Glomeribacter gigasporarum' is preferentially expressed during the symbiotic phases of its host mycorrhizal fungus. *Molecular Plant–Microbe Interactions* **22**: 302–310.

Bonfante P. 2014. The endless tale of endobacteria: a conversation with Paola Bonfante. *Trends in Plant Science* **19**: 744–746.

Bonfante P, Anca IA. 2009. Plants, mycorrhizal fungi, and bacteria: a network of interactions. *Annual Review in Microbiology* **63**: 363–383.

Bonfante P, Genre A. 2015. Arbuscular mycorrhizal dialogues: do you speak 'plantish' or 'fungish'? *Trends in Plant Science* **20**: 150–154.

Bosch TC, McFall-Ngai MJ. 2011. Metaorganisms as the new frontier. *Zoology* **114**: 185–190.

Bulgarelli D, Schlaeppi K, Spaepen S, Ver Loren van Themaat E, Schulze-Lefert P. 2013. Structure and functions of the bacterial microbiota of plants. *Annual Reviews in Plant Biology* **64**: 807–838.

Case RM, Eisner D, Gurney A, Jones O, Muallem S, Verkhratsky A. 2007. Evolution of calcium homeostasis: from birth of the first cell to an omnipresent signalling system. *Cell Calcium* **42**: 345–350.

Chiapello M, Martino E, Perotto S. 2015. Common and metal-specific proteomic responses to cadmium and zinc in the metal tolerant ericoid mycorrhizal fungus Oidiodendron maius. *Metallomics* **7**: 805–815.

Contreras-Shannon V, McAlister-Henn L. 2004. Influence of compartmental localization on the function of yeast NADP$^+$-specific isocitrate dehydrogenases. *Archives of Biochemistry and Biophysics* **423**: 235–246.

Cox J, Mann M. 2011. Quantitative, high-resolution proteomics for data-driven systems biology. *Annual Review of Biochemistry* **80**: 273–299.

Cunningham K, Fink G. 1996. Calcineurin inhibits VCX1-dependent H^+/Ca^{2+} exchange and induces Ca^{2+} ATPases in *Saccharomyces cerevisiae*. *Molecular & Cellular Biology* **16**: 2226–2237.

Cunningham KW. 2011. Acidic calcium stores of *Saccharomyces cerevisiae*. *Cell Calcium* **50**: 129–138.

Debska K, Bogatek R, Gniazdowska A. 2012. Protein carbonylation and its role in physiological processes in plants. *Biochemistry* **58**: 34–43.

DerMardirossian C, Bokoch GM. 2005. GDIs: central regulatory molecules in Rho-GTPase activation. *Trends in Cellular Biology* **15**: 356–363.

Ebbole DJ. 1998. Carbon catabolite repression of gene expression and conidiation in *Neurospora crassa*. *Fungal Genetics & Biology* **25**: 15–21.

Fedorova M, Bollineni RC, Hoffmann R. 2014. Protein carbonylation as a major hallmark of oxidative damage: update of analytical strategies. *Mass Spectrometry Reviews* **33**: 79–97.

Feussner I, Polle A. 2015. What the transcriptome does not tell – proteomics and metabolomics are closer to the plants' patho-phenotype. *Current Opinion in Plant Biology* **26**: 26–31.

Frey-Klett P, Burlinson P, Deveau A, Barret M, Tarkka M, Sarniguet A. 2011. Bacterial–fungal interactions: hyphens between agricultural, clinical, environmental, and food microbiologists. *Microbiology and Molecular Biology Reviews* **75**: 583–609.

Fujimura R, Nishimura A, Ohshima S, Sato Y, Nishizawa T, Oshima K, Masahira Hattori M, Narisawa K, Ohtaa H. 2014. Draft genome sequence of the betaproteobacterial endosymbiont associated with the fungus *Mortierella elongata* FMR23-6. *Genome Announcements* **2**: e01272-14.

Ghignone S, Salvioli A, Anca I, Lumini E, Ortu G, Petiti L, Cruveiller S, Bianciotto V, Piffanelli P, Lanfranco L *et al.* 2012. The genome of the obligate endobacterium of an AM fungus reveals an interphylum network of nutritional interactions. *ISME Journal* **6**: 136–145.

Haider S, Pal R. 2013. Integrated analysis of transcriptomic and proteomic data. *Current Genomics* **14**: 91–110.

Iraqui I, Kienda G, Soeur J, Faye G, Baldacci G, Kolodner RD, Huang ME. 2009. Peroxiredoxin Tsa1 is the key peroxidase suppressing genome instability and protecting against cell death in *Saccharomyces cerevisiae*. *PLoS Genetics* **5**: e1000524.

Karunakaran R, Ramachandran VK, Seaman JC, East AK, Mouhsine B, Mauchline TH, Prell J, Skeffington A, Poole PS. 2009. Transcriptomic analysis of Rhizobium leguminosarum Biovar viciae in symbiosis with host plants *Pisum sativum* and *Vicia cracca*. *Journal of Bacteriology* **191**: 4002–4014.

Keller B, Mühlenkamp M, Deuschle E, Siegfried A, Mössner S, Schade J, Griesinger T, Katava N, Braunsdorf C, Fehrenbacher B *et al.* 2015. *Yersinia enterocolitica* exploits different pathways to accomplish adhesion and toxin injection into host cells. *Cellular Microbiology* **17**: 1179–1204.

Lackner G, Hertweck C. 2011. Impact of endofungal bacteria on infection biology, food safety, and drug development. *PLoS Pathogens* **7**: e1002096.

Lanfranco L, Novero M, Bonfante P. 2005. The mycorrhizal fungus *Gigaspora margarita* possesses a CuZn superoxide dismutase that is up-regulated during symbiosis with legume hosts. *Plant Physiology* **137**: 1319–1330.

Lee W-J, Hase K. 2014. Gut microbiota-generated metabolites in animal health and disease. *Nature Chemical Biology* **10**: 416–424.

Levine RL, Williams JA, Stadtman ER, Shacter E. 1994. Carbonyl assays for determination of oxidatively modified proteins. *Methods in Enzymology* **233**: 346–357.

Lin K, Limpens E, Zhang ZH, Ivanov S, Saunders DGO, Mu DS, Pang E, Cao H, Cha H, Lin T *et al.* 2014. Single nucleus genome sequencing reveals high similarity among nuclei of an endomycorrhizal fungus. *PLoS Genetics* **10**: e1004078.

Liu Y, Gianinazzi-Pearson V, Arnould C, Wipf D, Zhao B, Van Tuinen D. 2013. Fungal genes related to calcium homeostasis and signalling are upregulated in symbiotic arbuscular mycorrhiza interactions. *Fungal Biology* **117**: 22–31.

Locato V, Gadaleta C, De Gara L, De Pinto MC. 2008. Production of reactive species and modulation of antioxidant network in response to heat shock: critical balance for cell fate. *Plant, Cell & Environment* **31**: 1606–1619.

Lounifi I, Arc E, Molassiotis A, Job D, Rajjou L, Tanou G. 2013. Interplay between protein carbonylation and nitrosylation in plants. *Proteomics* **13**: 568–578.

Lumini E, Bianciotto V, Jargeat P, Novero M, Salvioli A, Faccio A, Bécard G, Bonfante P. 2007. Presymbiotic growth and sporal morphology are affected in the arbuscular mycorrhizal fungus *Gigaspora margarita* cured of its endobacteria. *Cell Microbiology* **9**: 1716–1729.

Maier T, Guell M, Serrano L. 2009. Correlation of mRNA and protein in complex biological samples. *FEBS Letters* **583**: 3966–3973.

Mathew M, Lopanik N. 2014. Host differentially expressed genes during association with its defensive endosymbiont. *Biology Bulletin* **226**: 152–163.

Minard KI, McAlister-Henn L. 2001. Antioxidant function of cytosolic sources of NADPH in yeast. *Free Radical Biology and Medicine* **31**: 832–843.

Mondo SJ, Toomer KH, Morton JB, Lekberg Y, Pawlowska TE. 2012. Evolutionary stability in a 400-million-year-old heritable facultative mutualism. *Evolution* **66**: 2564–2574.

Moran NA, Bennett GM. 2014. The tiniest tiny genomes. *Annual Review in Microbiology* **68**: 195–215.

Moscatiello R, Sello S, Novero M, Negro A, Bonfante P, Navazio L. 2014. The intracellular delivery of TAT-aequorin reveals calcium-mediated sensing of environmental and symbiotic signals by the arbuscular mycorrhizal fungus *Gigaspora margarita*. *New Phytologist* **203**: 1012–1020.

Mühlenkamp M, Oberhettinger P, Leo JC, Linke D, Schütz MS. 2015. *Yersinia* adhesin A (YadA) – beauty & beast. *International Journal of Medical Microbiology* **305**: 252–258.

Naito M, Morton JB, Pawlowska TE. 2015. Minimal genomes of mycoplasma-related endobacteria are plastic and contain host-derived genes for sustained life within Glomeromycota. *Proceedings of the National Academy of Sciences, USA* **112**: 7791–7796.

Novero M, Faccio A, Genre A, Stougaard J, Webb KJ, Mulder L, Parniske M, Bonfante P. 2002. Dual requirement of the *LjSym4* gene for mycorrhizal development in epidermal and cortical cells of *Lotus japonicus* roots. *New Phytologist* **154**: 741–749.

Pepe JC, Wachtel MR, Wagar E, Miller VL. 1995. Pathogenesis of defined invasion mutants of *Yersinia enterocolitica* in a BALB/c mouse model of infection. *Infection and Immunity* **63**: 4837–4848.

Pfeffer PE, Douds DD, Bécard G, Shachar-Hill Y. 1999. Carbon uptake and the metabolism and transport of lipids in an arbuscular mycorrhiza. *Plant Physiology* **120**: 587–598.

Ralser M, Walmelink MM, Kowald A, Gerisch B, Heeren G, Struys EA, Klipp E, Jakobs C, Breitenbach M, Lehrach H *et al.* 2007. Dynamic rerouting of the carbohydrate flux is key to counteracting oxidative stress. *Journal of Biology* **6**: 10.

Recorbet G, Abdallah C, Renaut J, Wipf D, Dumas-Gaudot E. 2013. Protein actors sustaining arbuscular mycorrhizal symbiosis: underground artists break the silence. *New Phytologist* **199**: 26–40.

Regelmann J, Schüle T, Josupeit FS, Horak J, Rose M, Entian KD, Thumm M, Wolf DH. 2003. Catabolite degradation of fructose-1,6-bisphosphatase in the yeast *Saccharomyces cerevisiae*: a genome-wide screen identifies eight novel GID genes and indicates the existence of two degradation pathways. *Molecular Biology of the Cell* **14**: 1652–1663.

Ruiz-Herrera J, León-Ramírez C, Vera-Nuñez A, Sánchez-Arreguín A, Ruiz-Medrano R, Salgado-Lugo H, Sánchez-Segura L, Peña-Cabriales JJ. 2015. A novel intracellular nitrogen-fixing symbiosis made by *Ustilago maydis* and *Bacillus* spp. *New Phytologist* **207**: 769–777.

Ruzicka D, Chamala S, Barrios-Masias FH, Martin F, Smith S, Jackson LE, Brad Barbazuk W, Schachtman DP. 2013. Inside arbuscular mycorrhizal roots –molecular probes to understand the symbiosis. *Plant Genome* **6**: 13.

Salvioli A, Chiapello M, Fontaine J, Lounes Hadj-Sahraoui A, Grandmougin-Ferjani A, Lanfranco L, Bonfante P. 2010. Endobacteria affect the metabolic profile of their host *Gigaspora margarita*, an arbuscular mycorrhizal fungus. *Environmental Microbiology* **12**: 2083–2096.

Salvioli A, Ghignone S, Novero M, Navazio L, Venice F, Bagnaresi P, Bonfante P. 2016. Symbiosis with an endobacterium increases the fitness of a mycorrhizal fungus, raising its bioenergetic potential. *ISME Journal* **10**: 130–144.

Salvioli A, Zouari I, Chalot M, Bonfante P. 2012. The arbuscular mycorrhizal status has an impact on the transcriptome profile and amino acid composition of tomato fruit. *BMC Plant Biology* **27**: 12–44.

Samalova M, Meyer AJ, Gurr SJ, Fricker MD. 2014. Robust anti-oxidant defences in the rice blast fungus *Magnaporthe oryzae* confer tolerance to the host oxidative burst. *New Phytologist* **201**: 556–573.

Schwanhäusser B, Busse D, Li N, Dittmar G, Schuchhard T, Wolf J, Chen W, Selbach M. 2011. Global quantification of mammalian gene expression control. *Nature* **473**: 337–342.

Selvaraj SK, Periandythevar P, Prasadarao NV. 2007. Outer membrane protein A of *Escherichia coli* K1 selectively enhances the expression of intercellular adhesion molecule-1 in brain microvascular endothelial cells. *Microbes and Infection* **9**: 547–557.

Sgobba A, Paradiso A, Dipierro S, De Gara L, de Pinto MC. 2015. Changes in antioxidants are critical in determining cell responses to short- and long-term heat stress. *Physiologia Plantarum* **153**: 68–78.

Singh S, Brocker C, Koppaka V, Chen Y, Jackson BC, Matsumoto A, Thompson DC, Vasiliou V. 2013. Aldehyde dehydrogenases in cellular responses to oxidative/electrophilic stress. *Free Radical Biology & Medicine* **56**: 89–101.

Snoek ISI, Steensma H. 2007. Factors involved in anaerobic growth of *Saccharomyces cerevisiae*. *Yeast* **24**: 1–10.

Timpel C, Zink S, Strahl-Bolsinger S, Schroppel K, Ernst J. 2000. Morphogenesis, adhesive properties, and antifungal resistance depend on the Pmt6 protein mannosyltransferase in the fungal pathogen *Candida albicans*. *Journal of Bacteriology* **182**: 3063–3071.

Tisserant E, Malbreil M, Kuo A, Kohler A, Symeonidi A, Balestrini R, Charron P, Duensing N, Frei dit Frey N, Gianinazzi-Pearson V *et al.* 2013. Genome of an arbuscular mycorrhizal fungus provides insight into the oldest plant symbiosis. *Proceedings of the National Academy of Sciences, USA* **110**: 20117–20122.

Toft C, Andersson SG. 2010. Evolutionary microbial genomics: insights into bacterial host adaptation. *Nature Reviews Genetics* **11**: 465–475.

Torres-Cortés G, Ghignone S, Bonfante P, Schüßler A. 2015. Mosaic genome of endobacteria in arbuscular mycorrhizal fungi: trans-kingdom gene transfer in an ancient mycoplasma–fungus association. *Proceedings of the National Academy of Sciences, USA* **112**: 7785–7790.

Valadi A, Granath K, Gustafsson L. 2004. Distinct intracellular localization of Gpd1p and Gpd2p, the two yeast isoforms of NAD^+-dependent glycerol-3-phosphate dehydrogenase, explains their different contributions to redox-driven glycerol production. *Journal of Biological Chemistry* **279**: 39677–39685.

Weids AJ, Grant CM. 2014. The yeast peroxiredoxin Tsa1 protects against protein-aggregate induced oxidative stress. *Journal of Cell Science* **127**: 1327–1335.

Wernegreen J. 2012. Strategies of genomic integration within insect–bacterial mutualisms. *Biological Bulletin* **223**: 112–122.

Wewer V, Brands M, Dörmann P. 2014. Fatty acid synthesis and lipid metabolism in the obligate biotrophic fungus *Rhizophagus irregularis* during mycorrhization of *Lotus japonicus*. *Plant Journal* **79**: 398–412.

Zheng X, Ji Y, Weng X, Huang X. 2015. RpoS-dependent expression of OsmY in *Salmonella enterica* serovar typhi: activation under stationary phase and SPI-2-inducing conditions. *Current Microbiology* **70**: 877–882.

Supporting Information

Additional supporting information may be found in the online version of this article.

Fig. S1 Venn diagrams.

Fig. S2 Protein carbonylation profiles of *Lotus japonicus* roots after mycorrhizal colonization with the B+ or B− line.

Fig. S3 Representative two-dimensional profiles of protein abundance and oxidation in B+Myc and B−Myc clover roots.

Table S1 Primers used for reverse transcription-quantitative polymerase chain reaction (RT-qPCR) analyses

Table S2 List of the fungal proteins identified by iTRAQ (isobaric tags for relative and absolute quantification) analysis

Table S3 List of the differentially expressed proteins in the B− line in comparison with the B+ line

Table S4 List of the differentially GR24-responsive proteins in the B− line in comparison with the B+ line

Table S5 Bacterial proteins differentially expressed in the B+GR24 sample in comparison with the B+ sample

Table S6 List of differentially carbonylated proteins in B−Myc in comparison with B+Myc

Methods S1 Supplemental experimental procedures.

Please note: Wiley Blackwell are not responsible for the content or functionality of any supporting information supplied by the authors. Any queries (other than missing material) should be directed to the *New Phytologist* Central Office.